Author(s): Havu, P. & Sillanpää, A. & Runeberg, N. & Tarus, J. & Seppälä, E. T. & Nieminen, Risto M.

Title: Effects of chemical functionalization on electronic transport in carbon nanobuds

Year: 2012

Version: Final published version

Please cite the original version:

Havu, P. & Sillanpää, A. & Runeberg, N. & Tarus, J. & Seppälä, E. T. & Nieminen, Risto M. 2012. Effects of chemical functionalization on electronic transport in carbon nanobuds. Physical Review B. Volume 85, Issue 11. 115446/1-9. ISSN 1550-235X (electronic). DOI: 10.1103/physrevb.85.115446.

Effects of chemical functionalization on electronic transport in carbon nanobuds

P. Havu,[1] A. Sillanpää,[2] N. Runeberg,[2] J. Tarus,[2] E. T. Seppälä,[3] and R. M. Nieminen[1]
[1]*Aalto University, School of Science and Technology, Department of Applied Physics, P.O. Box 11100, FI-00076 AALTO, Finland*
[2]*CSC IT Center for Science, Keilaranta 14, FI-02101 Espoo, Finland*
[3]*Nokia Research Center, Itämerenkatu 11-13, FI-00180 Helsinki, Finland*
(Received 7 December 2011; published 29 March 2012)

Carbon nanobuds form a class of hybrid structures consisting of carbon nanotubes onto which fullerene types of units are covalently grown. Due to higher electrophilicity and curvature of the fullerene moiety a carbon nanobud exhibits higher reactivity compared to a plain nanotube. In this paper we study how the electronic structure and transport properties of carbon nanobuds are affected by chemical modification. The studied model systems comprise carbon nanobuds that are chemically modified by attaching Li and F atoms as well as tetrathiafulvalene molecules. We use the density functional theory combined with Landauer-Büttiker electron transport formalism. According to the simulations, the attached units change the relative positions of the Fermi levels, creating a distinctive effect on the electronic transport properties along associated carbon nanotubes. In semiconducting nanotubes the change in the conductance is systematic and should be detectable in experiments. Hence, the carbon nanobuds are potential candidates for sensor applications.

DOI: 10.1103/PhysRevB.85.115446 PACS number(s): 73.63.Fg, 72.80.Rj, 71.15.−m

I. INTRODUCTION

Carbon nanotubes (CNTs) are of scientific and technological interest due to their many superior physical and chemical properties, for example, their outstanding electrical, optical, and thermal conductivities and mechanical strength.[1] However, the perfect crystalline structure, the honeycomb lattice, of CNTs, while being responsible for the excellent properties of the nanotubes, make them also chemically inert, especially in the case of single wall CNTs. By chemically functionalizing CNTs, one can make them more easily applicable for many technical applications, such as acting as a photovoltaic material, as a molecular sensor, etc.[1–4] However, usually the methods required for doing that are so invasive that they destroy the perfect structure of a CNT and thus its excellent properties. A carbon-based hybrid material has been proposed to circumvent the problem of how to retain the outstanding properties of a CNT while tailoring it for applications (e.g., by chemical doping). The novel material, the carbon nanobud (CNB),[5] consists of a CNT onto which chemically more active fullerenelike structures are covalently bonded during synthesis. The higher reactivity of the fullerene structure is rationalized by its higher curvature creating a higher strain compared to that of a CNT.

Since their discovery in 2007, the carbon nanobuds have attracted a fair amount of interest both in experimental and theoretical studies. It has been shown both experimentally and theoretically that the fullerene sites of a CNB are indeed more reactive and hence more readily functionalized than the nanotube part of it.[6] Theoretical simulations also show that the conductance of a nanobud depends on the details of its geometry. The existence of the fullerene moiety on the tube can alter the property of whether the CNT is metallic or a semiconductor.[7–11] Some of the nanobud geometries even generate an unpaired spin at the connection point of the fullerene part to the nanotube or to a graphene layer, causing the CNB to have a magnetic moment.[12,13]

Besides the many theoretical and experimental studies, there are still open questions left, especially regarding functionality of CNBs. Since one motivating property for introducing the CNB was its chemical activity, it is interesting to see how different absorbents on a CNB affect the electronic transport properties in it. In other words, is it possible to create by chemically functionalizing the reactive fullerene sites perturbations that can be detected as changes in measured properties along the associated tube parts? With a positive answer, it will be important if or when CNBs are used for developing, for example, molecular sensors.

Here we study theoretically the behavior of carbon nanobuds under chemical doping. In order to investigate mechanisms behind variation in conductance caused by attached molecules and atoms, we chose two extreme units that are known to act as strong electron donors or acceptors, Li and F atoms, respectively. While behaving either electronegatively (F) or electropositively (Li), we can study how these extreme ligands affect the charge redistribution between the fullerene part and the CNT part of a CNB. In addition to the extreme electron donors and acceptors, the Li and F atoms, we also study how a tetrathiafulvalene (TTF) ligand affects the charge distribution and conductance properties of the CNB. TTF is commonly used in C_{60}-fullerene chemistry due to its strong electron-donating property that can be utilized when developing, for example, molecular sensors, logic gates, switches, photovoltaic applications, etc.[14–17]

Due to the multitude of different ways the fullerene part can be attached to the tube, all the possible geometries of CNBs cannot be investigated. However, some of the configurations are motivated by the experimental transmission electron microscopy pictures.[5] Here, we have chosen four different model configurations of which three have fullerenelike units attached to (14,0) semiconductor CNTs with different "neck" structures joining them. The fourth model system consists of a fullerene structure fused to an (8,8) metallic CNT. In our model we assume that the distance between fullerene parts is long enough so that different fullerene parts do not interact with each other.

The calculations are performed using the density functional theory combined with the Landauer-Büttiker electron transport

formalism. Our simulations show that these chemically bonded units alter the conductance of a CNB by two mechanisms: by modifying the potential barriers at the nanotube and by moving the relative position of the Fermi level.

This paper is organized as follows. Section II presents briefly the density functional theory method combined with the electron transport formalism. Implementation of the gate potential is also presented in the section. In Sec. III the constructed model systems for the various hypothetical nanobud structures are described and their electronic structure and transport simulation results are presented. In Sec. IV effects of functionalization on the CNBs by doping them with Li and F atoms and a TTF molecule are studied. In Sec. V, the simulation results are combined and compared as a function of the gate potential. The paper is concluded in Sec. VI.

II. SIMULATION METHODS

The calculations are done based on the density functional theory using a FHI-aims implementation.[18] We use a PBE[19] exchange correlation functional and include van der Waals corrections.[20] The transport calculations are done using a Landauer-Büttiker formalism,[21,22] which is also implemented in the FHI-aims code. The methods are known to give accurate enough approximations and still work efficiently for large system sizes. In our calculations, we use a double numeric plus a polarization basis set of the numerical atom-centered orbital basis functions.

First the Kohn-Sham equations are iterated using a periodic supercell approximation. After the convergence, the system is embedded between semi-infinite nanotube leads for the transport calculations. The leads are connected to the ends of the CNT part of a carbon nanobud configuration.

The retarded Green's function of the system is calculated using nonreflecting open boundary conditions,

$$\left\{E - \hat{H}_0 - \sum_i \Sigma_i^r(E)\right\} G^r(\mathbf{r},\mathbf{r}';E) = \delta(\mathbf{r}-\mathbf{r}'), \qquad (1)$$

where $\hat{H}_0$ is the Hamiltonian of the CNB region and Σ_i^r are the so-called self-energies of the semi-infinite leads. In charge-doped systems, the boundary conditions are evaluated using plain nanotubes with the same relative charge doping densities as in the case of carbon nanobuds. From the G^r we can then evaluate the electronic transmission between leads one and two, connected to the tube ends, using

$$T(E)_{1-2} = \int_{\partial\Omega_1}\int_{\partial\Omega_1}\int_{\partial\Omega_2}\int_{\partial\Omega_2} d\mathbf{r}_1\, d\mathbf{r}_1'\, d\mathbf{r}_2\, d\mathbf{r}_2', \times \Gamma_1(\mathbf{r}_1,\mathbf{r}_1')\, G^r(\mathbf{r}_1',\mathbf{r}_2)\, \Gamma_2(\mathbf{r}_2,\mathbf{r}_2')\, G^a(\mathbf{r}_2',\mathbf{r}_1), \qquad (2)$$

where $i\Gamma_i = 2i\,\mathrm{Im}(\Sigma_i^r)$ and $\partial\Omega_{1-2}$ are the boundaries to the leads. G^a is the so-called advanced Green's function, here being the complex conjugate of G^r. Finally the conductance is calculated using the Landauer-Büttiker formula,

$$G = \frac{2e^2}{h}\int_{-\infty}^{\infty} T(E)\left\{-\frac{\partial f(E)}{\partial E}\right\} dE. \qquad (3)$$

At a lead connection point, a reference potential, $\epsilon_{\min}$, of the semi-infinite lead and the tube end of CNB is matched. The reference potential $\epsilon_{\min}$ in our all-electron calculations is the average of the smallest Kohn-Sham eigenvalues from the eigenstates localized to the atoms close to the connection of the carbon nanobud to the semi-infinite leads. Every eigenstate of the smallest eigenvalues in all-electron calculations is well localized to distinct atoms, thus making their determination easy by simply projecting to atom-centered basis functions. Green's function calculations for the semi-infinite leads are performed using both neutral and charged leads. However, in practice both cases give identical results for the CNB conductance, because since the potential levels of leads match with the levels of nanotube ends of CNB, the small differences in the charge densities between Green's functions of the lead (when charged) and the CNB do not affect the conductance (compared to the neutral case).

Similarly as, for example, in field-effect transistors (FETs), also in these nanostructures, a gate voltage can be utilized to change the electrostatic potential, and thus it can be used to control the electronic current by pulling or pushing electrons from/to the leads to/from a nanostructure area depending on the electrostatic potential it creates. While the dimensions of the nanostructure is small compared to a typical gate electrode, the change of the electrostatic potential can be assumed to affect the whole nanostructure area uniformly. This is analogous with the back gate structure in FETs, where the gate voltage affects from below an insulating surface layer. Hence, it can be justified to mimic the effect of the gate voltage inversely by adding electrons to the system or removing them, solving the system at equilibrium, and measuring the potential. However, since we use the periodic supercell approximation for solving the Kohn-Sham equations, the size of the supercell can affect the local charge density, and thus the magnitude of the gate potential. This may happen if the extra charges do not occupy only local states but extend over the whole nanostructure. While we are interested in the trend of the effect of the gate potential and use practically the same size for the supercells, this should not matter. However, for the sake of comparison analysis, and usability and reproducibility of the results, we have defined the gate potential E_{gate} as

$$E_{\mathrm{gate}} = E_{\mathrm{Fermi}} - \epsilon_{\min} - E_0, \qquad (4)$$

where E_{Fermi} is the Fermi level of the carbon nanobud system and $\epsilon_{\min}$ is the reference potential level introduced above for the transport calculations. Here $\epsilon_{\min}$ represents the relative bottom energy of the system used for comparisons of the Fermi level changes. The potential E_0 of a charge neutral system sets the zero level for the gate potential E_{gate}.

III. PRISTINE NANOBUDS

A. The geometry of carbon nanobuds

The detailed structures of the CNBs are not easily and clearly shown in the experiments available, but it seems that the sizes and shapes of the fullerenelike parts, "buds," and the fullerene-nanotube connections, "necks," appear in various forms.[23,24] Statistical size measurements on the basis of high-resolution transmission electron microscopy (HR-TEM) images suggest that the majority of fullerenes consists of derivatives from C_{42} and C_{60}. The "buds" in the CNB samples

have been characterized also by their sizes based on scanning electron microscopy (SEM) analyses. The size distribution indicates that "buds" of the size of a C_{60} fullerene are most abundant, roughly 25%,[5] but there are also significant amounts of smaller buds, compatible with, for example, the size of a smaller C_{42} fullerene.

There are several theoretical calculations studying the possible structures of C_{60} carbon nanobuds,[7,8,10] and they can be classified in two main types of geometries: either a (nearly) perfect fullerene cage that is covalently bonded to a CNT via a few carbon bonds[8,10,11] or the fullerene part is merged to the CNT by a thicker, hollow neck.[7,10]

In this work we concentrate only on model systems that are based on the C_{60} derivatives. In order to study the effect of the geometry on the transport properties of CNBs, we have created several model structures, including both of the major CNB types, perfect fullerene balls (A) and hollow necks (B–D), as shown in Fig. 1. The CNT parts of the CNBs A–C are semiconducting (when as separate tubes, but also as a part of the carbon nanobud configurations as we shall see below) (14,0) structures, whereas the tube in D is (8,8) metallic, similarly as separately but also as a part of the CNB. Apart from the structure A, the geometries have been created by removing atoms from the tube and a C_{60} molecule in a symmetric fashion to generate five, six, seven, or eight rings and exclusively three coordinated carbon atoms in the neck area. The structures A, B, and D are similar to the ones in the paper by Nasibulin *et al.*,[5] and the model A is also close to the CNB used in the simulations by Wu *et al.*[8,11]

The geometries have been optimized using DFT until forces are less than $1e$-2 eV/Å. The supercell is 30-Å long for the structures with a (14,0) nanotube and 25-Å long for the structure with an (8,8) tube. A vacuum layer of 20 Å has been used.

We have not attempted to study the kinetic stability of the model structures in more detail, that would merit a separate investigation, but we have used two ways to look at their relative energies: first, the total formation energy relative to the same number of free atoms divided by the number of atoms in the configuration; and another one based on

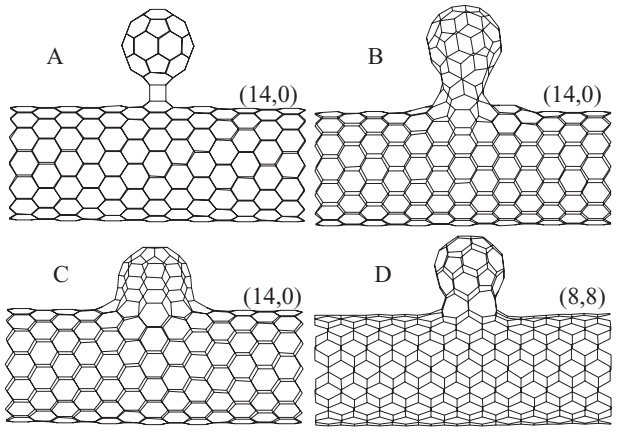

FIG. 1. Four different carbon nanobud geometries used in the numerical simulations: three (A–C) consisting of a fullerene connected to a semiconducting (14,0) CNT tube, and one (D) to an (8,8) metallic tube.

TABLE I. The relative energies of the model CNB structures, calculated in two ways: (a) according to Eq. (5) and (b) formation energy relative to free atoms divided by the total number of atoms in the configuration.

		Energy, ΔE (eV)	
CNB	N in Eq. (5)	(a)	(b)
A	60	0.3798	−44.5065
B	60	5.9068	−44.4943
C	34	7.3744	−44.5062
D	48	8.1960	−44.4907

$$\Delta E = E_{\mathrm{CNB}} - E_{\mathrm{CNT}} - \frac{N}{60} E_{\mathrm{C_{60}}}, \tag{5}$$

where E_{CNB} is the total energy of a CNB, E_{CNT} is the total energy of a pristine CNT of the same length and size as the nanotube in the CNB, $E_{\mathrm{C_{60}}}$ is the total energy of a fullerene, and N is the number atoms in the bud part of the CNB. The latter definition approximates the strain energies in the necks of the model configurations although it is not straightforward since different necks have different numbers of atoms. The energies for the used structures using both definitions are given in Table I.

A fused C_{60} and a nanotube are thermodynamically less favorable than separate intact molecules and therefore the formation energy relative to them is positive. However, based on Eq. (5), the structure A is predicted to have the smallest strain, which is due to it being closest to the intact separate molecules (see Table I). Nevertheless, the structure might not be kinetically very stable as only two bonds hold otherwise independently stable moieties together. In the other structures, the strain is larger, but the formation energy of structure C is practically the same as for A. We interpret this to derive from a smaller number of fullerenelike atoms which compensates for the strain. Overall, the formation energies of all the structures relative to free atoms are of the same order and we consider all the models as possible structures.

B. Charge transport properties of pristine nanobuds

We start by analyzing charge transmission properties of nonfunctionalized, pristine carbon nanobuds of the structures A–D described in the previous section at charged and neutral states. The electron transmission curves and the density of states (DOS) are shown for the configurations in Fig. 2. Note that in the simulations the minimum number of charges that is added to the system is two, in order to avoid any problems related to spin polarization.

The charge neutral results agree well with the calculation results reported in literature.[9,11] The local electron states in the fullerene parts of the carbon nanobuds are seen as additional sharp spikes of DOS compared to pure CNTs. They are located at different energies for different CNBs, but all the semiconducting systems A, B, and C have additional ones inside the CNT energy gap. A similar outcome is reported also for the carbon nanobud systems by He *et al.*[10] Additionally, the metallic configuration D has sharp spikes of density of

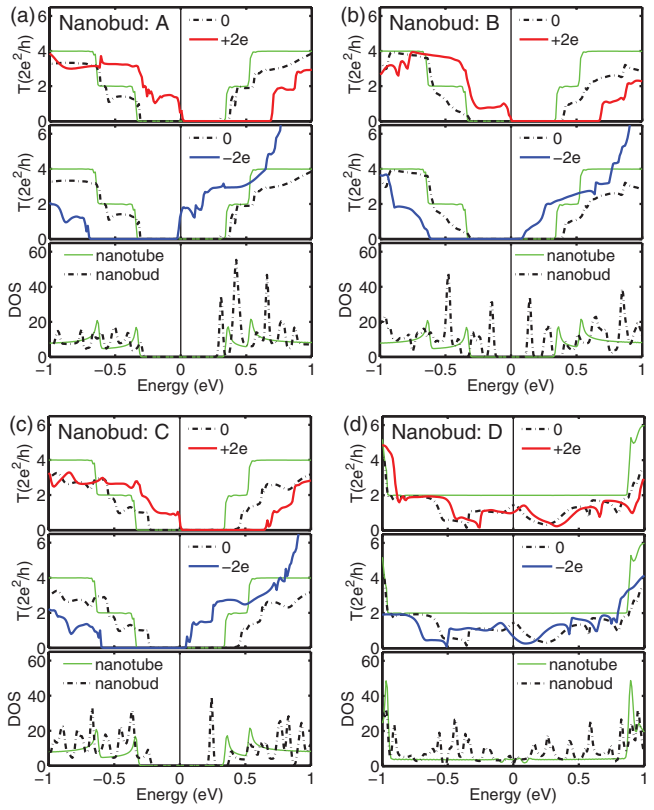

FIG. 2. (Color online) The transmission curves of the carbon nanobud configurations (a) A, (b) B, (c) C, and (d) D as neutral systems (upmost and middle panels) and as charged systems ($+2e$ in the upmost panels, $-2e$ in the middle panels). The lowest panels show the density of states for the charge neutral systems and for CNTs as a reference. The green thin lines in all of the figures (a)–(d) and all the panels are as reference for the corresponding pure, charge neutral CNTs, semiconducting (14,0) in (a)–(c), and metallic (8,8) in (d). The Fermi level is at 0 eV.

states close to the Fermi level, as seen also in earlier studies,[9] staying metallic as it has been reported elsewhere, too.[7]

In our model configurations, the nanotube parts are long enough, so that (with the periodic boundary conditions) the bud parts are fairly well separated from their mirror images, and thus the local states of the fullerene parts do not interact or correlate with each other. This is visible in the density of states (Fig. 2) as the additional spikes compared to the CNTs stay well separated from the Fermi level in the energy gap, and the systems do not conduct, except naturally in the case of the metallic CNT (configuration D). The local states can be visualized in the charge density figures (Fig. 3), too. There, all the fullerene parts of the carbon nanobuds bear a small overall negative charge (blue). Simultaneously, the necks of the carbon nanobuds (the connection area of the bud parts to the tube parts) are somewhat positively charged (red). In simulations reported in the literature both positively and negatively charged fullerene parts of CNBs are observed,[8] and it is likely that there are some dependencies on the geometrical details to the charge distribution of a CNB.

The charge relocations between the CNT part and the bud part can also be seen as a shift of the Fermi level, especially in the semiconducting configurations (A–C) (see DOS panels in Fig. 2). Here, the Fermi level is defined to be in the middle of the energy gap and when a CNB has additional occupied or unoccupied states in the energy gap (compared with the corresponding pristine CNT) their positions define the new location for the Fermi level. The character of the fullerene part of pulling electrons from the nanotube part makes the Fermi level of the joint CNB move down in energy when compared with the corresponding pure nanotube (light green lines in Fig. 2).

When the carbon nanobud systems are charged by adding or removing electrons to/from the systems, the charges do not localize only in the fullerene parts of the carbon nanobuds but spread quite uniformly to the nanotubes, too (see the left panels in Fig. 3). Since also in the nanotube side of a fullerene-nanotube connection (neck) of a CNB are found local states, a better way to visualize the conduction properties of a system is the position of its Fermi level; see transmission curves in Fig. 2. In Fig. 2 the DOS curves are given only for charge neutral systems for the clarity reasons, but their movements are easy to imagine. In the cases of semiconducting carbon nanobuds (configurations A–C), when electrons are removed (the system p-doped), the edges of the conduction bands of the carbon nanobuds (that are effectively the same edges as found in the corresponding pure carbon nanotubes) move to the Fermi level, causing the systems to conduct. Instead, if electrons are added to the systems (n-doped), then the conduction bands move only closer to the Fermi level (in the cases of carbon nanobud configurations B and C) without conduction, because the extra electrons occupy the local states of the nanobuds. The nanobud configuration A, the geometry with a nearly isolated fullerene cage connected to a CNT, behaves quite similarly to a pristine carbon nanotube. There the first unoccupied local state

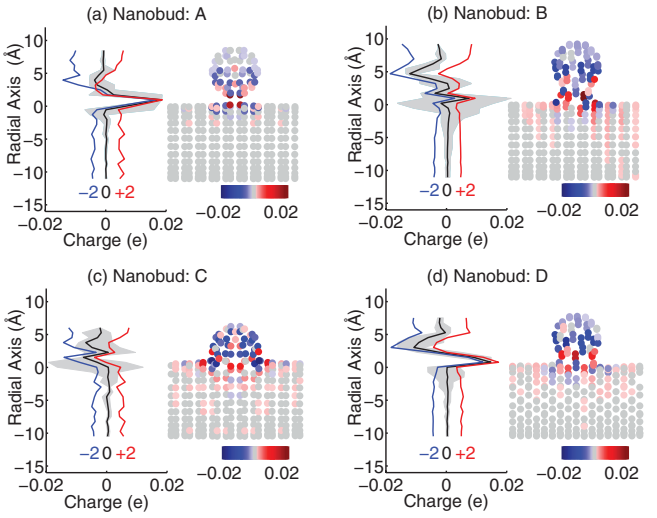

FIG. 3. (Color) At right of each figure, the Hirschfeld charge analysis[25] for different carbon nanobud geometries A–D in (a)–(d), respectively, at charge neutral states. At left, the average charge (averaged over the other two coordinates) is projected to an axis of the radial direction of the nanotube for the charge neutral as well as for $-2e$ and $+2e$ charged systems. The gray areas in the projections mark the maxima and minima of the charges at the planes with the same radial coordinates in the charge neutral systems.

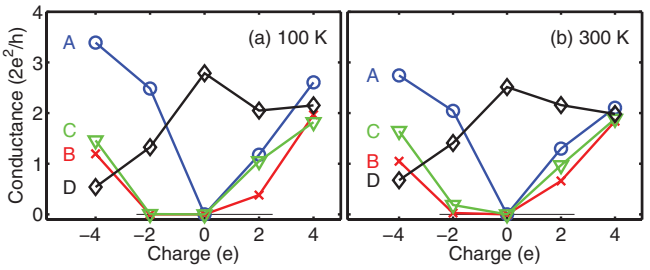

FIG. 4. (Color online) The conductance values for the carbon nanobud configurations A (blue circles), B (red crosses), C (green triangles), and D (black diamonds) as a function of the added/removed charges in the system. The Fermi broadening is used for the temperatures (a) 100 K and (b) 300 K.

is close to the conduction band, and the extra electrons move the Fermi level to the band, causing the system to conduct. However, since the kinetic stability of the carbon nanobud geometry A can be questioned, one can summarize that the kinetically stable semiconducting carbon nanobuds are easier to *p*-dope than *n*-dope.

In semiconductors, at finite temperature it is sufficient if the conduction band is close to the Fermi level to make the system conduct, because the electrons can have enough energy to hop into the conduction band. By using Fermi broadening in the electron transmission curves, one can estimate the conductance values at finite temperatures. The conductance values for different charged nanobuds are collected in Fig. 4 at temperatures 100 and 300 K. The conductance values are not sensitive to the used temperatures, as the results are quite similar for both temperatures. Here the asymmetry of conductances of the *p*-doping and *n*-doping can still be seen as the configurations B and C conduct better with $+2e$ charges than with $-2e$. With the charges $+4e$ and $-4e$ the differences have evened out. Trivially, in the metallic configuration D as strong changes in the Fermi levels are not seen as in the semiconducting systems A, B, and C. However, also there the spiky structure of the DOS has an effect on the conductance, as the exact positions of the peaks move to and from the Fermi level.

Besides the Fermi level movements, the conductance is also affected by the potential walls, that exist in the paths of the charge carriers within the carbon nanobuds. The walls are different for the charge neutral and the charged systems, which can be seen as different shapes in the electron transmission curves. The effect is smaller than the changes in the Fermi level of the CNBs, but still noticeable.

IV. FUNCTIONALIZATION OF THE NANOBUDS

A. Geometry of functionalized nanobuds

Since the main motivation for this study is to investigate the sensitivity of the CNBs to chemical doping and how that could be detected, a straightforward way to execute that is to attach atoms to the systems and investigate their effects on the DOS and conductivity. As explained in Introduction, stronger curvature due to the carbon atom five rings in the fullerene parts of carbon nanobuds make them more reactive than the pristine, rolled sheets of graphene in the carbon nanotubes. Therefore, adatoms attach more easily on the fullerene parts of CNBs than on the nanotubes.[6] Also the necks, the fullerene-nanotube connection areas of CNBs, could be active due to their other than six ring structures. However, there curvature is opposite the one in the bud part, and space for additional molecules or atoms could be too tight, due to steric repulsion. In any case, the neck as a possible location for functionalization cannot be totally neglected, especially in case adatoms can penetrate into the CNB and attach to its wall from inside. Anyhow, in this paper we use as a possible functionalization location only the top of the fullerene part of a CNB, as motivated by the paper by Raula *et al.*[6]

To study the effect of functionalization we add and withdraw electrons to/from the nanobud by using Li (electron donor) and F (electron acceptor) adatoms. It is known that Li and F atoms can be attached fairly easily to nanotubes, too.[26] However, as explained above, since the aim of this paper is not to investigate the possible locations of the adatoms that have been investigated elsewhere,[6,27] we place the atoms directly on the top of the fullerene part. In all the systems we use an even number of adatoms. In part this is motivated by guaranteeing the safe handling of the spin polarization in the calculations but also as a reference to real functionalization reactions that typically result in two functional groups at the nanostructure surface in either an ortho or a para position. The former, the ortho position, separates the adatoms with one carbon bond along the vertex of two six membered rings, whereas the latter with three bonds in the same six membered ring. In order to discover trends we use two and 24 adatoms of each type to study the increasing polarization of the bud. The structures with 24 adatoms are created by placing the adatoms at the bud top followed by a geometry optimization.

In order to investigate the effect of more applicable molecules, and not only simple light atoms, we study the tetrathiafulvalene (TTF) molecule (Fig. 5) attached at the top of the bud of each CNB configuration. TTF is known as a strong electron donor in charge transfer complexes.[14–16] Its derivative has also been covalently attached to C_{60} in fullerene chemistry, thus making it as a viable candidate molecule for carbon nanobud chemistry, as well. The TTF molecule is attached in an ortho fashion, in the vertex of two six-rings, as explained above. In the structure A there is a six-ring at the bud top, whereas, for example, in the structure C at the top there is a five-ring and therefore the TTF molecule is positioned "radially" from the bud top, and thus the TTF configurations vary from each other somewhat, as will be seen later.

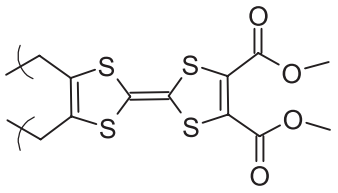

FIG. 5. A schematic picture of the tetrathiafulvalene molecule, which has been used to probe the effects of functionalization. The bonds at left are connected to the bud part of the carbon nanobud in an ortho position, (i.e., to neighboring carbon atoms).

B. Charge transport of carbon nanobuds with Li and F atoms

Li and F adatoms change the local electronic structure of the bud part of the carbon nanobud, as can be seen in the charge density figures [Figs. 6(a) and 6(c)] for the carbon nanobud configuration B with two added Li and F atoms, respectively. This is in contrast to the case, presented in Sec. III, where extra electrons were added or removed from the system, and the extra negative or positive charges spread quite uniformly to the system. The fact that the two adatoms, Li and F atoms, change the charge densities only in the bud parts is the same for all the studied CNB configurations A–D (Fig. 6 for configuration B is a representative case). While the bud parts of the carbon nanobuds bear a net negative charge, both Li and F atoms cause the neck to stay positively charged, even when Li pushes and F pulls electrons to/from the bud part. However, when polarization is taken to an extreme with 24 adatoms [see Figs. 6(b) for Li and 6(d) for F], then the charge effects are also seen in the CNT part.

The adatoms have fairly big effects on the local electronic structure of the nanobuds, shown in Fig. 7 for configurations B and C. The results for the other configurations A and D are similar and not shown for compactness. As a reference, for the F atoms we show two configurations for the placement of the atoms, ortho and para. In the DOS close to the Fermi level clear changes are seen in all the cases. However, the changes are less dramatic in the electron transmission curves that stay almost unaffected for most of the carbon nanobud geometries. In a few cases relatively large shifts in the Fermi level are observed, such as in the configuration C with two Li atoms [Fig. 7(c)]. This may be not due to a property of the carbon nanobud itself, but more related to the positioning of the adatoms in the bud parts, as illustrated with the two different F atom positioning in the nanobud configuration C: While the

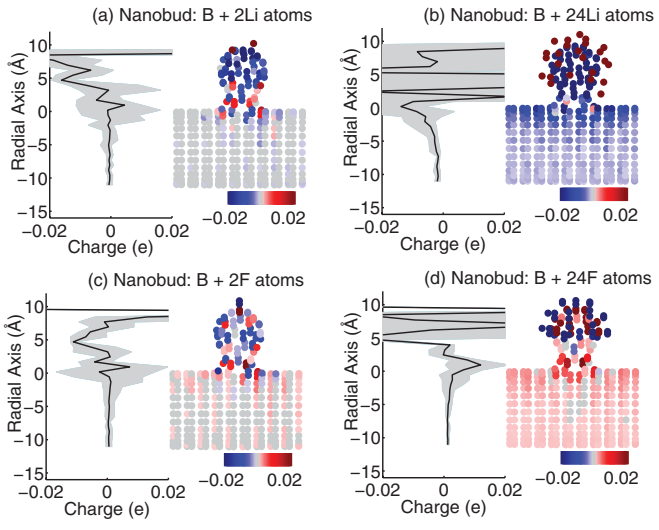

FIG. 6. (Color) Hirschfeld charge analysis for the carbon nanobud configuration B with added Li [two in (a) and 24 in (b)], and F [two in (c) and 24 in (d)] atoms. The diagrams on the left of all the figures show the average of the charges along the radial axis (averaged over the other two coordinates) and gray areas mark the maxima and minima of the charge values of the planes at the corresponding radial coordinates.

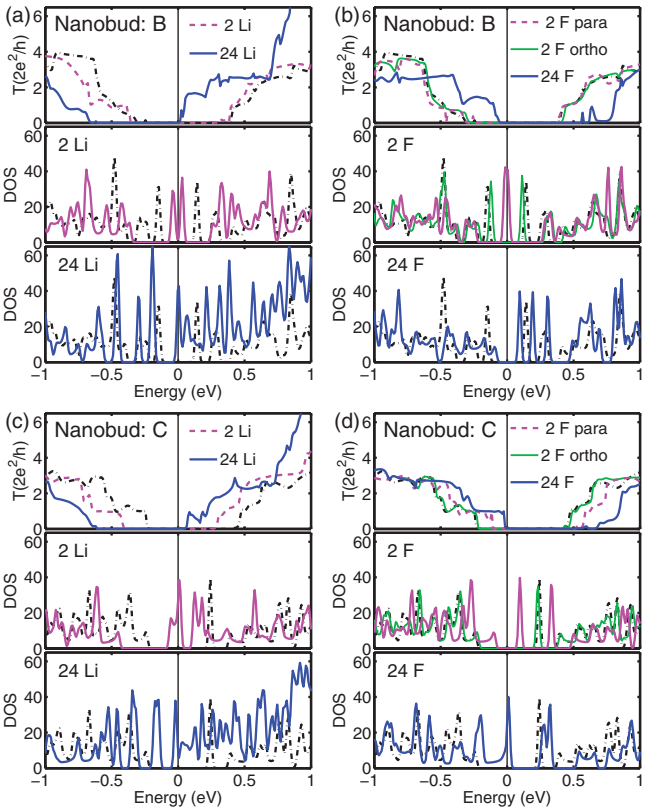

FIG. 7. (Color online) The electron transmission curves (upmost panels) and density of states (with two adatoms in the middle panels and 24 atoms in the lowest panels) for the nanobud configuration B, with attached (a) Li and (b) F atoms, and C, with attached (c) Li and (d) F atoms. The F atoms are positioned as two different configurations, ortho and para, in the transport and electronic structure simulations. The dashed black lines show the transmission and the DOS curves of the corresponding pristine CNB configurations.

F atoms in the para position shift the Fermi level quite a lot, the ortho position has a very minor effect [Fig. 7(d)].

While two Li and F atoms cause only small differences in conductivity of the carbon nanobuds compared with the pristine ones, a larger number of atoms have much more noticeable effects as shown in Fig. 8. The minor effect with two small adatoms may be due to the small volume of

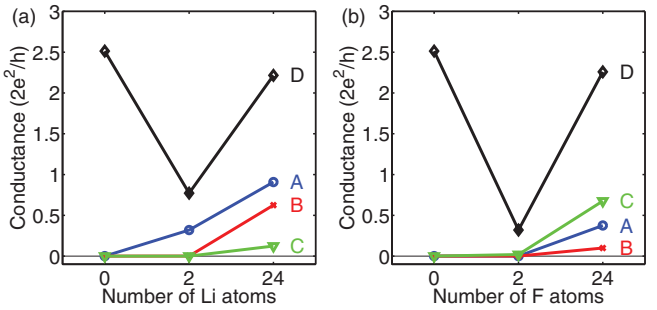

FIG. 8. (Color online) The conductance values of different carbon nanobud configurations A (blue circles), B (red crosses), C in para positions (green triangles), and D (black diamonds) as a function of the number of (a) Li and (b) F atoms with Fermi broadening at 300 K.

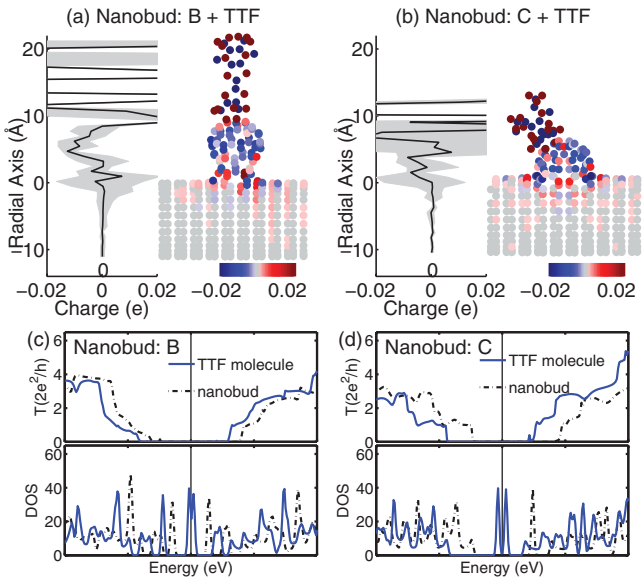

FIG. 9. (Color) The Hirschfeld charge distributions for nanobud configurations (a) B and (b) C with TTF molecules. The axes are the same as in Fig. 3. The transmission curves (upper panels) and the density of states (lower panels) of the nanobud configurations (c) B and (d) C with TTF molecules. The dashed black lines show the transmission and the DOS curves of the corresponding pure CNBs. Whether (a) or not (b) there is a six-ring at the bud top, the positioning of the TTF molecule on the bud differs substantially, as explained in Sec. IV A.

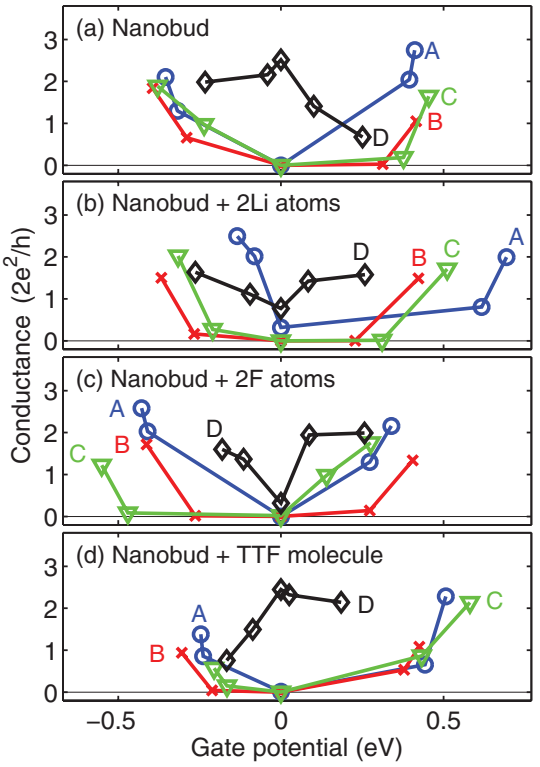

FIG. 10. (Color online) The conductance values of different carbon nanobud configurations A (blue circles), B (red crosses), C (green triangles), and D (black diamonds) as a (a) pristine CNB and with adatoms, (b) two Li and (c) two F atoms, and (d) a single TTF molecule, as a function of the gate potential. The Fermi broadening at 300 K is used.

the extra electrons they can donate or accept, whereas the larger number of atoms have a much bigger total volume of electrons for donation or acceptance. For the applicability of the carbon nanobuds, as, for example, a sensor, it is interesting to notice that the direction of conductance changes in all the semiconducting nanobud configurations (A–C) is the same with both Li and F atoms and both ortho and para positions: increasing. However, in the case of the metallic nanobud configuration D it does not happen. Generally, the details in the electronic structure close to the Fermi level have big effects on the conductance values. Adatoms change the structure of DOS, which then changes conductance in a nonsystematic way in metallic systems. It is also quite likely that different metallic CNBs behave very differently, and thus applicability of the metallic carbon nanobuds as sensors can be left in doubt.

C. Charge transport of carbon nanobuds with TTF molecules

The charge transfer from Li atoms are local to the fullerene part of the CNB. Similarly, also in the case of a more applicable molecule TTF, its addition results in a negative charge in the bud part, as can be seen in Figs. 9(a) and 9(c) for CNB configurations B and C. This can also be seen in the shapes of the transmission curves [Figs. 9(b) and 9(d)] that remain unaffected after attaching TTF molecules. While the TTF molecule changes the electronic structure of the bud part quite a bit (see the DOS curves in Fig. 9), it hardly affects the underlying nanotube part. The clear shift of the Fermi level can be seen in the transmission curves of Fig. 9, but the change is not large enough to bring the conduction band to the Fermi level. Therefore, a carbon nanobud functionalized with a TTF molecule will not make a semiconducting CNT to conduct without applied gate voltage.

V. EFFECT OF GATE VOLTAGE

In order to compare the transport results of the different CNB configurations as pristine, with different adatoms, and with the TTF molecule, and also to plot them using more generally applicable units, the conductance is shown as a function of the gate potential in Fig. 10. The gate potential is calculated from electrostatic potential levels of charged and neutral self-consistent calculations using Eq. (4) as described in Sec. II. One should note that the sign of the gate potential is opposite the sign of the added charge (used in Fig. 4) as the added charge is compensated with the oppositely signed background potential (i.e., the gate potential), due to the fact that the total charge in the actual calculation always has to vanish and the system must be neutral.

When the gate potential is increased (or decreased), the semiconducting carbon nanobud configurations A–C start to conduct at approximately the same gate potential V_c. When the adatoms are included, then the variations in V_c are increased. However, on average the electron donors (Li, TTF) shift V_c up in potential, whereas the electron acceptor F atoms move it down. Hence the perturbations that increase or decrease the number of electrons in the carbon nanobuds, should be detectable in the nanotubes of the semiconducting CNBs. The

difference relative to the specific geometry A–C of a CNB is smaller with TTF than with Li or F atoms. In addition, the effect is stronger with positive doping (F) than with a negative doping (Li). This is due to the fact that the bud parts of the pristine carbon nanobuds tend to attract electrons by themselves and with electro-positive doping the attraction is enhanced.

The effect of functionalized carbon nanobuds on transport behavior of metallic CNTs is more complicated than in the semiconducting ones. The density of states close to the Fermi level is spiky, and the detailed position of the spikes depends on the specific structure of a nanobud. Even if a response of doping can be measured along the tube, the behavior is most likely not systematic, and in the worst case, the changes average out to zero.

VI. CONCLUSIONS

In this paper, the effects of F and Li adatoms and a covalently bonded TTF molecule on the electronic structure and transport properties of carbon nanobuds as four different configurations are simulated. In the simulations, the adatoms affect the electronic structure of the carbon nanobuds. The effect, however, stays mainly in the fullerene part of the carbon nanobud and does not extend to the related nanotube, and thus the potential wall of the nanotube part of a CNB stays almost the same. On the other hand, the relative position of the Fermi level moves, and changes in the conductance of semiconducting carbon nanobuds can be measured.

For applicability of carbon nanobuds as sensors, it is not sufficient only that the CNBs are easy to dope with atoms or molecules, they should also have systematic and noticeable effects on the charge carrier transport properties along the related carbon nanotubes. In many applications, CNTs are used as a mat or net, or as a so-called *bucky paper*; this is likely to be the case for carbon nanobuds, as well. Therefore, an application may consist of several carbon nanobuds, and thus fine details will be averaged out. In order not to average interesting measurement values out to zero, but to maximize their effects, and hopefully to sum them to a more macroscopic value than is typical from nanodevices, the trend of the values should be in the same direction in all the individual carbon nanobuds. That is luckily the case, as the trend in all the studied semiconducting CNBs A–C is quite the same, as shown in Fig. 10. On the other hand, in the metallic configuration of the CNB the effect is dependent on small details in a nonsystematic manner and derived values from different metallic configurations may cancel each other. Thus, as with many other CNT applications, as for example, in field-effect transistors where metallic nanotubes either short-circuit the devices or at least decrease the on-off ratio of the current, also in the devices and applications based on carbon nanobuds, a method is needed to remove the metallic CNBs.

While it is shown in this paper that (semiconducting) CNBs are sensitive, in a systematic way, to perturbations, adatoms, and molecules, and are able to behave as sensors themselves, one should bear in mind that in practical sensor applications the sensors are often exposed to air and other molecules, causing problems for the sensors' capability of detecting specific molecules (i.e., their selectivity). Even if different molecules can be distinguished by different effects caused by the electron transport properties along the nanotubes, it is likely that a more practical way is to use the nanobud as a template for more selective molecules, specifically defined to detect certain molecules. This would increase the selectivity, as well as refresh the capability of a sensor. Then only the molecule(s) with which a CNB is functionalized acts as a sensor. Furthermore, in that case, the effects should be measurable along the CNT part of the CNB. This may be difficult in case the inherent electro-negative property of the fullerene part is not satisfied, as happens here without applied gate potential with a TTF molecule and when there are only two F or Li atoms.

ACKNOWLEDGMENTS

Financial support from Finnish Technology Agency TEKES through the Nokia NanoRadio project is acknowledged. We also thank Ilya Anoshkin, Vladimir Ermolov, Janne Raula, and Javad Hashemi for useful discussions.

[1] M. S. Dresselhaus, G. Dresselhaus, and P. C. Eklund, *Science of Fullerenes and Carbon Nanotubes* (Academic Press, San Diego, 1996).

[2] G. Bottari, G. de la Torre, D. M. Guldi, and T. Torres, Chem. Rev. **110**, 6768 (2010).

[3] S. Latil, S. Roche, and J.-C. Charlier, Nano Lett. **5**, 2216 (2005).

[4] R. Chitta, A. S. D. Sandanayaka, A. L. Schumacher, L. D'Souza, Y. Araki, O. Ito, and F. D'Souza, J. Phys. Chem. C **111**, 6947 (2007).

[5] A. G. Nasibulin, P. V. Pikhitsa, H. Jiang, D. P. Brown, A. V. Krasheninnikov, A. S. Anisimov, P. Queipo, A. Moisala, D. Gonzalez, G. Lientschnig, A. Hassanien, S. D. Shandakov, G. Lolli, D. E. Resasco, M. Choi, D. Tomanek, and E. I. Kauppinen, Nature Nanotech. **2**, 156 (2007).

[6] J. Raula, M. Makowska, J. Lahtinen, A. Sillanpää, N. Runeberg, J. Tarus, M. Heino, E. T. Seppälä, H. Jiang, and E. I. Kauppinen, Chem. Mater. **22**, 4347 (2010).

[7] T. Meng, C.-Y. Wang, and S.-Y. Wang, Phys. Rev. B **77**, 033415 (2008).

[8] X. Wu and X. C. Zeng, ACS Nano **2**, 1459 (2008).

[9] J. A. Fürst, J. Hashemi, T. Markussen, M. Brandbyge, A. P. Jauho, and R. M. Nieminen, Phys. Rev. B **80**, 035427 (2009).

[10] H. Y. He and B. C. Pan, J. Phys. Chem. C **113**, 20822 (2009).

[11] P. Zhao, P. J. Wang, Z. Zhang, M. J. Ren, and D. S. Liu, Physica B: Condensed Matter **405**, 2097 (2010).

[12] X. Zhu and H. Su, Phys. Rev. B **79**, 165401 (2009).

[13] M. Wang and C. M. Li, Phys. Chem. Chem. Phys. **13**, 5945 (2011).

[14] J. Oh, S. Roh, W. Yi, H. Lee, and J. Yoo, J. Vac. Sci. Technol. B **22**, 1416 (2004).

[15] N. Martin, L. Sanchez, M. A. Herranz, B. Illescas, and D. M. Guldi, Acc. Chem. Res. **40**, 1015 (2007).

[16] D. Canevet, M. Salle, G. Zhang, D. Zhang, and D. Zhu, Chem. Comm. **2009**, 2245 (2009).

[17]M. Bendikov, F. Wudl, and D. F. Perepichka, Chem. Rev. **104**, 4891 (2004).
[18]V. Blum, R. Gehrke, F. Hanke, P. Havu, V. Havu, X. Ren, K. Reuter, and M. Scheffler, Comput. Phys. Commun. **180**, 2175 (2009).
[19]J. P. Perdew, K. Burke, and M. Ernzerhof, Phys. Rev. Lett. **77**, 3865 (1996).
[20]A. Tkatchenko and M. Scheffler, Phys. Rev. Lett. **102**, 073005 (2009).
[21]R. Landauer, Philos. Mag. **21**, 863 (1970).
[22]M. Büttiker, Phys. Rev. Lett. **57**, 1761 (1986).
[23]Y. Tian, D. Chassaing, A. G. Nasibulin, P. Ayala, H. Jiang, A. S. Anisimov, and E. I. Kauppinen, J. Am. Chem. Soc. **130**, 7188 (2008).
[24]Y. Tian, D. Chassaing, A. G. Nasibulin1, P. Ayala, H. Jiang, A. S. Anisimov, A. Hassanien, and E. I. Kauppinen, Phys. Status Solidi B **245**, 2047 (2008).
[25]F. L. Hirshfeld, Theor. Chim. Acta **44**, 129 (1977).
[26]W. Koh, J. I. Choi, K. Donaher, S. G. Lee, and S. S. Jang, ACS Appl. Mater. Interfaces **3**, 1186 (2011).
[27]A. Sillanpää, N. Runeberg, J. Tarus, and E. T. Seppälä (unpublished).